

# From 3-DoF to 6-DoF: New Metrics to Analyse Users Behaviour in Immersive Applications

Silvia Rossi, *Student Member, IEEE*, Irene Viola *Member, IEEE*, Laura Toni *Member, IEEE*, and Pablo Cesar *Senior Member, IEEE*

**Abstract**—This work focuses on enabling user-centric immersive systems, in which every aspect of the coding-delivery-rendering chain is tailored to the interactive users. Understanding the actual interactivity and behaviour of those users is still an open challenge and a key step to enable such a user-centric system. Our main goal is to enable user behavioural analysis in the case of 6 degree-of-freedom (DoF) systems by extending the applicability of existing behavioural methodologies adopted for studying user behaviour in 3-DoF settings. Specifically, we deeply analyse 6-DoF navigation patterns with comparisons to the 3-DoF counterpart. Then, we define new metrics aimed at better modelling users similarities in a 6-DoF system. We validate and test our solutions on real navigation paths of users while displaying dynamic volumetric media in 6-DoF Virtual Reality conditions. To show the flexibility and generality of our proposed metrics, we also test their performance on navigation trajectories collected in a 6-DoF Augmented Reality settings. Our results show that metrics that consider both user position and viewing direction better perform in detecting user similarity while navigating in a 6-DoF system. Having easy-to-use but robust metrics that underpin multiple tools and answer the question “how do I detect if two users look at the same content?” open the gate to new solutions for a user-centric system.

**Index Terms**—Point Cloud, User Analysis, Data Clustering, 6-DoF, Immersive Reality, Virtual Reality, Augmented Reality.

## I. INTRODUCTION

IMMERSIVE reality technology has revolutionised how users engage and interact with media content, going beyond the passive paradigm of traditional video technology, and offering higher degrees of presence and interaction in a virtual environment. Depending on the enabled locomotion functionalities in the 3D space, immersive environments can be classified as 3- or 6-Degrees-of-Freedom (DoF). In the first scenario, the de-facto multimedia content is the *omnidirectional* or *spherical video*, which represents an entire 360° environment on a virtual sphere. The viewer is fully immersed in a virtual space where they can navigate and interact thanks to an immersive device – typically an head-mounted display

Silvia Rossi and Laura Toni are with the Department of Electrical & Electrical Engineering, UCL, London (UK), e-mails: s.rossi@ucl.ac.uk, ltoni@ucl.ac.uk.

Irene Viola is with Centrum Wiskunde & Informatica (CWI), Amsterdam (The Netherlands), e-mail: irene.viola@cwi.nl.

Pablo Cesar is with Centrum Wiskunde & Informatica (CWI), Amsterdam (The Netherlands), and also with TU Delft, Delft (The Netherlands), e-mail: P.S.Cesar@cwi.nl.

This work has been carried out while Silvia Rossi was doing her internship at Centrum Wiskunde & Informatica (CWI), Amsterdam (The Netherlands).

Manuscript received April 19, 2005; revised August 26, 2015.

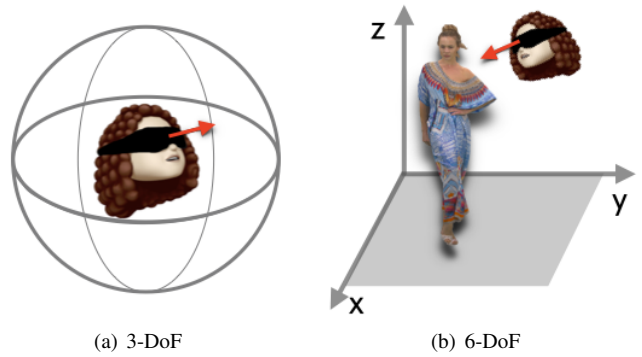


Fig. 1. Viewing paradigm in 3- and 6-DoF VR.

(HMD), which enables to display only a portion of the environment around him/herself, named *viewport*. Moreover, the user is virtually positioned at the centre of a sphere as shown in Fig. 1 (a). The media is displayed from an *inward* position, and the viewer can interact with the content only by changing the viewing direction (*i.e.*, by looking up/down or left/right or tilting the head side to side). In a 6-DoF system, the user can also change viewing perspective by moving (e.g., walking, jumping) inside the virtual space. The scene is therefore populated by *volumetric objects* (*i.e.*, meshes or point clouds) which are observed from an *outward* position (Fig. 1 (b)). This extra degree of freedom brings the virtual experience even closer to reality: a higher level of interactivity makes the user feels more immersed and present within the virtual environment [1].

Despite their differences, the common denominator of both interactive systems is the viewer as an active decision-maker of the displayed content. This active role of the user defines the *user-centric* era, in which content preparation, streaming, and rendering need to be tailored to the viewer interaction to remain bandwidth-tolerant whilst meeting quality and latency criteria. Media codecs need to be optimised in such a way that the quality experienced by the user is maximised [2], [3]. Analogously, to ensure high-quality content and smooth navigation, but remaining bandwidth-tolerant [4], [5], [6], streaming should be tailored to users interactivity. The latter however is highly dependent on the user navigation within the content which is not known *a priori*. Here is an urgent need to understand, analyse and predict users behaviour [7], [8], [9].

Thanks to the large availability of public datasets [10], [11], [12], [13], user navigation in 3-DoF immersive systems has been deeply investigated [14], [15], showing the importance of analysing and detecting key behavioural aspects in interactive

(user-centric) systems. However, the 6-DoF counterpart is not yet considered in the literature apart from some few cases [16], [17], [18]. Moreover, due to the change in the viewing paradigm (from inward to outward) and due to a higher degree of freedom in 6-DoF, current studies in 3-DoF cannot be directly applied to 6-DoF domains, as shown in our previous work [19]. Filling this gap by providing new tools for users analysis in 6-DoF is the main goal of this paper.

In this paper, we focus on extending the applicability of clustering methods to investigate users similarity (i.e., users sharing common behaviours while interacting with the content) in a 6-DoF environment. Specifically, clustering techniques usually rely on pairwise similarity metrics, and at the moment there is no a proposed metric to measure the interactivity similarity between two users in 6-DoF. Starting from state-of-the-art clustering developed for 3-DoF [20], we describe the main limitations of the tool when extended to 6-DoF, and we propose a new methodology for overcoming those limitations. First, we define the user navigation pattern in 6-DoF, highlighting the main differences and novelty with respect to 3-DoF. Then, we define the exact user similarity metric, which we will be considering as our ground truth. Given its computational complexity, after an exhaustive study, we propose a simpler and yet reliable proxy for it. More concretely, we define and compare 8 different similarity metrics which are based on different *distance features* (i.e., user positions in the 3D space, user viewing directions) and *distance measurements* (i.e., Euclidean, Geodesic distance). We validate and test our proposed similarity metrics on a publicly available dataset of navigation trajectories collected in a 6-DoF Virtual Reality (VR) scenario [5]. Results have shown that similarity metrics based on different distance features are promising solutions to correctly detecting users with a similar behaviour while experiencing volumetric content. Finally, we validate the proposed tool by testing it on navigation trajectories collected in a different setting, a 6-DoF Augmented Reality (AR) scenario [18]. Similarities among users are detected as well in this new interactive setting, showing that the proposed metric is general to be efficient in multiple interactive systems with 6-DoF.

In conclusion, our work contributes to the overall open problem of behavioural analysis in a 6-DoF system, with the following main contributions:

- formal definition of user trajectory and ground-truth user similarity (in terms of overlap of the display content) in 6-DoF, formally highlighting the main difference between 6-DoF and 3-DoF;
- an exhaustive analysis of different metrics capturing users trajectory similarity (in terms of distance on the plane or from the object) and the ability to approximate the ground truth. This analysis based on 6-DoF VR trajectories reveals the only position on the floor is not sufficient to characterise the user behaviour and the viewing direction cannot be neglected;
- a case study of behavioural analysis in an AR system via a state-of-the-art clustering tool using our proposed similarity metrics.

The remainder of this article is organised as follows: related

works on user behavioural analysis in both 3-DoF and 6-DoF systems are reported in Section II. The main challenges of detecting behavioural similarities in a 6-DoF system and the importance of having a tool that approximates such similarities are described in Section III. Our proposed similarity metrics are described and validated on real navigation trajectories collected in a 6-DoF VR settings in Section IV and Section V, respectively. In Section VII, a case of study is presented to show the applicability of our proposed metrics also to an 6-DoF AR setting. Our results are further discussed in Section VIII, highlighting possible directions for future work. Conclusions are summarised in Section IX.

## II. RELATED WORK

### A. User Behaviour in 3-DoF environment

The user navigation within a 3-DoF environment has been intensely analysed from many perspectives. Many studies have been focused on psychological investigations of user engagement and presence correlated to movements within the spherical content. In [21], a study from a large scale experiment (511 users and 80 omnidirectional videos) showed the positive correlation between lower interactivity level and higher engagement level (strong focus on few points of interest). Similarly, a correlation between the perceived sense of presence and the interactivity level was detected in [22], with more random exploratory interactions for less immersed (and hence less engaged) users.

However, none objective metric to properly quantify and characterise the user behaviour has been presented in these works. To further understand how people observe and explore 360° contents, many public datasets of navigation trajectories have been made available. Those datasets usually come with statistical analysis aimed at capturing average users behaviour, as a function of maximum and average angular speeds under various video segment lengths [10] or eye fixation distribution [11]. A deeper analysis was presented in [13] where the dataset has been analysed through a clustering algorithm presented in [20], specifically built to have in the same cluster users who similarly explore 360° content. The analysis validated previous understanding that movies with few focus of attention lead to higher engagement, in this case, shown by users sharing strong similarities and hence collected into few and high-populated clusters. However, behavioural analysis based on such clustering tool mainly provides a general idea of similarity among viewers without offering however a quantitative metric. To overcome such limitation, authors in [15], showed the benefit of studying spatio-temporal trajectories by information theory metrics, and thus the possibility of identifying and quantifying behavioural aspects. Key outcomes from this quantitative analysis were the study of similarities between users when watching the same content, but also the similarity of a given user when watching diverse content. The importance of these behavioural insights has been then exploited in different VR applications. For instance, authors in [23] proposed a scalable prediction algorithm for user navigation, which considered previous navigation patterns while in [24] an hybrid approach has been presented based

on both dominant user behaviour (detected via a clustering approach) and the video content. Moreover, the analysis and understanding of user navigation in a VR environment has shown promising results also in determining the mental health issues of subjects (e.g., anxiety, eating disorders, depression) and their treatment [25], [26].

### B. User Behaviour in 6-DoF environment

Extending such behavioural analysis to a 6-DoF environment is not straightforward, due to the change in the viewing paradigm (from inward to outward) and to the addition of translation in 3D space. In the past, user navigation in 6-DoF scenarios was studied in the context of locomotion and display technology for CAVE environments [27], [28]. A Cave Automatic Virtual Environment (CAVE) system is an immersive room on which walls and floor are projected the video content and viewers are free to move inside [29]. For instance, the study in [27] focused on the task performance analysis in terms of completion time and correct actions. Authors in [28] compared instead the effect of two different immersive platforms such as CAVE and HMD on the user navigation. More traditional metrics, such as angular distance and linear velocity, alongside completion time, were also used to compare different navigation controllers (*i.e.*, joystick-based vs head-controlled navigation) in 6-DoF [30]. In detail, authors showed the superiority of head-controlled techniques, allowing more sense of presence and better control with less discomfort in the navigation. While the aforementioned analysis tools are highly informative to summarise the interaction of users within a 6-DoF environment, they usually fail in providing other key insights: which users navigate similarly, and which are the dominant interaction behaviour among users.

Recently, the focus has been put on subjective quality assessment based on different coding techniques of volumetric content, both static [16] and dynamic [17], [5]. These studies present a preliminary statistical analysis of user movements in terms of mean angular velocity, most displayed areas of the content showing an influence in the navigation due to the perceived content quality, and a preference to visualise the volumetric object from a close and frontal perspective. This last finding was also confirmed in a behavioural navigation analysis while consuming volumetric video content by an AR mobile application [18]. Here, viewers movements were analysed in terms of distribution on the floor, viewing angles, and relative distance from the content. Finally, a behavioural analysis of user navigating in 6-DoF social VR movie has been presented in [31]. An investigation on how users are affected by virtual characters and narrative elements of the movie has been conducted through objective metrics, showing a more static behaviour when an interactive task was requested, and more exploratory movements during dialogues. All these preliminary studies are based on traditional metrics for behavioural analysis, which consider only one user feature at the time, either position on the floor or viewing direction but not together, suffering from the major shortcomings highlighted before. In this paper, we aim to overcome these limitations by proposing a generalisable and efficient tool for detecting similar viewers while experiencing 6-DoF content.

## III. CHALLENGES

In this work, our main goal is to define a new pairwise metric able to capture the (dis)similarity between two 6-DoF users (in terms of displayed content). This metric needs to be reliable and yet simple to compute. In the following, we first define our assumption of similarity among users while navigating in a 6-DoF environment. Then, we propose an exact user similarity metric highlighting its limitations, and therefore the need to find a simpler and reliable proxy for it. Finally, we show the advantages of having a similarity metric for behavioural analysis via a clique-based clustering approach presented in [20], which identified users who are attending the same portion of an omnidirectional content in a 3-DoF system. This clustering technique relies on a pairwise similarity metric, and thus, having a proper metric also for 6-DoF system would extend the applicability of this state-of-the-art tool.

### A. User Similarity in 6-DoF

We are interested in analysing user behaviour, assuming that users interact similarly when they *observe the same volumetric content*. The user behaviour can be identified by the spatio-temporal sequences of their movements within the virtual environment, namely *navigation trajectories*.

In a 3-DoF scenario, the trajectory of a generic user  $i$  can be formally denoted by the sequence of the user's viewing direction over time  $\{p_1^i, p_2^i, \dots, p_n^i\}$  where  $p_t^i$  is the centre of the viewport projected on the immersive content (*i.e.*, spherical video) at timestamp  $t$ . The point  $p$  can be represented in spherical coordinates by  $[\theta, \phi, r]$  where  $\theta \in [0, 2\pi]$  is the azimuth angle (or longitude),  $\phi \in [0, \pi]$  the polar angle (or latitude), and  $r$  is the distance between the point (viewport center projected on the immersive content) and the origin (user position). In a 3-DoF scenario, users are positioned at the centre of the spherical content; thus,  $r$  is constant during the interaction. As a consequence, the viewport centre alone is highly informative of the user behaviour and can be used as a proxy of viewport overlap among users [20]. In particular, the geodesic distance has been proved as a reliable similarity metric such that low value indicates high similarity between 3-DoF users.

In a 6-DoF setting, the distance between the user and immersive content can change over time due to the added degrees of freedom. Thus, the more degrees of freedom are given to the user, the more challenging becomes the system and the description of user navigation within it. The viewport centre alone is no more sufficient to characterise the user behaviour in a 6-DoF scenario. Fig. 2 shows an example of two users navigating in a 6-DoF system. In the bottom part of the figure, there are navigation trajectories of two users  $i$  and  $j$  projected on a 2-D domain (*i.e.*, floor). Each point  $x_t$  represents the spatial coordinates (*i.e.*, [x,y,z]) on the floor of viewers while each associated vector symbolises the viewing direction. In the top part of Fig. 2, we have instead a snapshot of a specific time instant  $t$ . In more detail, the shaded triangular areas represent the *viewing frustum* per user, which indicates the region within the user viewport, and  $r_t$  is the distance between the user and the volumetric content. We have also

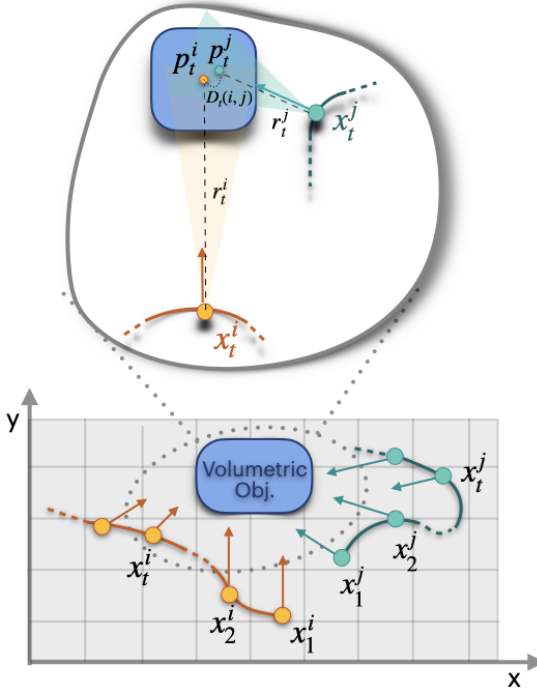


Fig. 2. An example of 6-DoF trajectories projected in a 2D domain for user  $i$  and  $j$ . In the circle, a snapshot at time  $t$  where coloured triangles represent viewing frustum per user.

depicted the viewport centre  $p_t$  projected on the displayed volumetric object. Given the two users  $i$  and  $j$  at time  $t$ , in the case of  $r_t^i \gg r_t^j$ , the user  $j$  (very close to the object) is visualising a very focused and detailed part of it; conversely, user  $i$  is pointing to the same area but from a much further distance, thus she/he is experiencing the content differently with less defined details. Despite this difference, the small distance  $D_t(i, j)$  between viewport centres  $p_t^i$  and  $p_t^j$  might suggest a high similarity (*i.e.*, high viewport overlap) between the corresponding users, which does not reflect the reality in the case of  $r_t^i \gg r_t^j$ . Thus in this scenario, we cannot rely on the viewport centre only to characterise the user behaviour. The distance  $r$  and the spatial coordinates on the virtual floor  $x$  are also needed. Given the above notation, we can formally define the navigation trajectory for a generic 6-DoF user  $i$  as  $\{(x_t^i, p_t^i, r_t^i), (x_2^i, p_2^i, r_2^i), \dots, (x_n^i, p_n^i, r_n^i)\}$ . This information is crucial to define a simple similarity metric among users in this new setting.

### B. Overlap Ratio as the ground-truth metric

Since we are interested in capturing viewers that are attending similar volumetric content at the same time instance, the straightforward measure that could show this behaviour is the overlap among viewports. Given two users  $i$  and  $j$  described above in Fig. 2 (top part), we denote their displayed viewport as  $\mathcal{S}_t^i$  and  $\mathcal{S}_t^j$ , respectively, defined as the set of points of the volumetric content falling within their viewing frustum. Then, we denote the overlap set by  $\mathcal{S}_t^i \cap \mathcal{S}_t^j$ , defined as the portion of points displayed by both users. Equipped with the above notation, we can now introduce a key metric for the analysis: the *overlap ratio*  $O(i, j)$ . This is defined as the cardinality of the overlap set, normalised by the cardinality of the set

containing all points of the volumetric content visualised by both users. More formally, the overlap ratio in a specific time  $t$  is:

$$O_t(i, j) = \frac{|\mathcal{S}_t^i \cap \mathcal{S}_t^j|}{|\mathcal{S}_t^i \cup \mathcal{S}_t^j|} \quad (1)$$

where  $\mathcal{S}_t^i$  and  $\mathcal{S}_t^j$  are the displayed viewport of users  $i$  and  $j$ , respectively. The higher is the overlap ratio, the higher is the similarity between users, and vice versa. Even if this metric is exact and a clear indicator of how much similar users are with respect to their displayed content, its evaluation is not trivial as it is intensely time-consuming. For instance, the overlap ratio between two users requires 0.8986 seconds per frame on average on an Intel R machine with CPU E5-4620 at 2.10 GHz; the operation needs to be computed for all the possible combinations of users, leading to a large overhead which does not meet requirements for real-time and scalable applications. A new measure is thus needed to perform clustering in near real-time. In the rest of the paper, we will use this metric as the ground truth of overlap among users, and we investigate the use of different weights as a proxy for viewport overlap.

### C. Clustering as a tool for behavioural analysis

Being able to assess users similarities in an objective way might be crucial for different applications such as behavioural analysis. As shown in [20], a clique-based clustering algorithm is used to detect users with similar behaviour. This requires a reliable graph to be constructed in such a way that only the nodes that identify similar users (*i.e.*, who are displaying the same portion of the content) are connected. Equipped with such a meaningful graph, the clique-based clustering identifies optimal sub-graphs of all inter-connected nodes, ensuring the identification of the largest cluster of users all sharing a large viewport overlap. In more detail, given a set of users who are experiencing the same content, we can represent their movements in a time-window  $T$  as a set of graphs  $\{\mathcal{G}_t\}_{t=1}^T$ . Each unweighted and undirected graph  $\mathcal{G}_t = \{\mathcal{V}, \mathcal{E}_t, \mathbf{A}_t\}$  represents behavioural similarities among users at time  $t$ , where  $\mathcal{V}$  and  $\mathcal{E}_t$  denote the node and edge sets of  $\mathcal{G}_t$ , respectively. Each node in  $\mathcal{V}$  corresponds to a user interacting with the content. Each edge in  $\mathcal{E}_t$  connects neighbouring nodes defined by the binary adjacency matrix  $\mathbf{A}_t$ . Assuming that users are connected if they are displaying similar content, we can formally define the adjacency matrix  $\mathbf{A}_t$  as follow:

$$\mathbf{A}_t(i, j) = \begin{cases} 1, & \text{if } w_t(i, j) \leq G_{th} \\ 0, & \text{otherwise.} \end{cases} \quad (2)$$

where  $w_t(i, j)$  is a similarity metric between user  $i$  and  $j$  and  $G_{th}$  is a thresholding value. On this final graph, the clique-based clustering algorithm can be applied to identify a set of users all connected (*i.e.*, clique), and therefore with similar behaviour. In [20], this graph construction is based on a pairwise similarity metric specifically for the 3-DoF trajectories.

Identifying a generic and reliable metric  $w(i, j)$  that approximates behavioural similarities among users who experience a 6-DoF content is a key step to enable user behavioural analysis via tools proposed for 3-DoF scenario and the focus on the next section.

TABLE I  
DEFINITION OF DISTANCE FEATURES AND MEASUREMENTS.

Symbol	Definition
$x$	user position on the VR floor
$p$	viewport center projected on the volumetric content
$r$	relative distance between user and volumetric content
$L(\cdot, \cdot)$	difference of relative distance between two users
$E(\cdot, \cdot)$	Euclidean distance
$G(\cdot, \cdot)$	Geodesic distance

#### IV. PROPOSED METRICS

In this section, we present eight similarity metrics and we provide an exhaustive study to understand which one approximates at the best the viewport overlap. Those metrics are expressed as a function of various *distance features* and *measurements* considering either users position on the floor ( $x$ ) or users viewing direction in terms of viewport centre projected on the volumetric content ( $p$ ) or both. Thus, we divide the metrics in two groups: *single-feature* and *multi-feature* metrics. Table I defines the distance features and measurements that we consider, while Table II summarises our proposed similarity metrics.

##### A. Single-feature metrics to assess users similarity

The first set of similarity metrics are based on one single feature (*i.e.*, the distance of either viewport centres on the volumetric content or users on the floor). For the sake of notation, in the following, we omit the temporal parameter  $t$ . We model the similarity functions via radial basis function kernel, and specifically the Gaussian kernel [32] defined as follows:

$$k_{\alpha}^{(D)}(i, j) = e^{-\alpha D(i, j)} \quad (3)$$

where  $D(i, j)$  is the distance between two generic users  $i$  and  $j$ , while  $\alpha > 0$  is a parameter to better regularise the distance. This distance can be evaluated in multiple ways. The first two similarity metrics  $w_1$  and  $w_2$  are based on the location of users in the virtual space with respect to the virtual object or other viewers. The former is based on the Euclidean distance  $E(x^i, x^j)$  between user  $i$  and  $j$  on the virtual floor, while  $w_2$  considers the difference of users relative distance to the centroid of the displayed content,  $L = ||r^i - r^j||$ . Specifically, we define them as follows:

$$w_1 = e^{-\alpha E(x^i, x^j)} = k_{\alpha}^{(E)}(x^i, x^j); \quad (4)$$

$$w_2 = e^{-\alpha ||r^i - r^j||} = k_{\alpha}^{(L)}(r^i, r^j). \quad (5)$$

The metrics  $w_3$  and  $w_4$  are instead based on the distance between the two viewport centres of user  $i$  and user  $j$  projected on the volumetric content. To take into account the heterogeneous shape of the volumetric content, this distance in  $w_3$  is evaluated in terms of the Geodesic distance  $G(p^i, p^j)$  while in  $w_4$  in terms of the Euclidean distance  $E(p^i, p^j)$ . More formally, they are defined as:

$$w_3 = k_{\alpha}^{(G)}(p^i, p^j) = e^{-\alpha G(p^i, p^j)} \quad (6)$$

$$w_4 = k_{\alpha}^{(E)}(p^i, p^j) = e^{-\alpha E(p^i, p^j)}. \quad (7)$$

##### B. Multi-feature metrics to assess users similarity

As emerged in our preliminary study [19], both user viewing direction and position on the virtual floor are relevant to detect similar behaviour among users. Therefore, the last set of proposed similarity metrics considers a combination of the above features. In detail,  $w_5$  and  $w_6$  are composed by the pairwise Euclidean distance in the virtual space  $E(x^i, x^j)$  and the difference of user relative distance to the volumetric content  $||r^i - r^j||$  but include also the distance of their viewport centres projected on the volumetric content in terms of Geodesic distance  $G(p^i, p^j)$  and Euclidean distance  $E(p^i, p^j)$ , respectively. More formally, we define the first:

$$w_5 = k_{\alpha}^{(E)}(x^i, x^j) \cdot k_{\beta}^{(L)}(r^i, r^j) \cdot k_{\gamma}^{(G)}(p^i, p^j) \\ = e^{-\alpha E(x^i, x^j)} \cdot e^{-\beta ||r^i - r^j||} \cdot e^{-\gamma G(p^i, p^j)}; \quad (8)$$

while the second weight is equal to:

$$w_6 = k_{\alpha}^{(E)}(x^i, x^j) \cdot k_{\beta}^{(L)}(r^i, r^j) \cdot k_{\gamma}^{(E)}(p^i, p^j) \\ = e^{-\alpha E(x^i, x^j)} \cdot e^{-\beta ||r^i - r^j||} \cdot e^{-\gamma E(p^i, p^j)}. \quad (9)$$

The preliminary analysis presented in [19] has also highlighted a correlation between the viewport overlap of two users and their relative distance from the volumetric content. The closer users are to the volumetric content, the smaller and more detailed is the portion of the displayed content; the farther they are, the bigger but with fewer details becomes the displayed portion. Thus, in the first case, the high overlap between displayed areas of two different users is more difficult. To take into consideration this behaviour, we model the relative distance via a hyperbolic tangent kernel. Given the relative distance  $r_i$  between the user  $i$  and volumetric content, we evaluate it as follows:

$$\eta(r_i) = \tanh(r_i). \quad (10)$$

As previously, metrics  $w_8$  and  $w_9$  are based on both user distance in the virtual floor  $E(x^i, x^j)$ , and on the volumetric content in terms of Geodesic distance  $G(p^i, p^j)$  and Euclidean distance  $E(p^i, p^j)$ , respectively. More formally, we define  $w_8$  as following:

$$w_8 = k_{\alpha}^{(E)}(x^i, x^j) \cdot \beta [\eta(r^i) + \eta(r^j)] \cdot k_{\gamma}^{(G)}(p^i, p^j) \\ = e^{-\alpha E(x^i, x^j)} \cdot \beta [\tanh(r_i) + \tanh(r_j)] \cdot e^{-\gamma G(p^i, p^j)}; \quad (11)$$

while  $w_9$  is:

$$w_9 = k_{\alpha}^{(E)}(x^i, x^j) \cdot \beta [\eta(r^i) + \eta(r^j)] \cdot k_{\gamma}^{(E)}(p^i, p^j) \\ = e^{-\alpha E(x^i, x^j)} \cdot \beta [\tanh(r_i) + \tanh(r_j)] \cdot e^{-\gamma E(p^i, p^j)}. \quad (12)$$

#### V. EXPERIMENTAL SETUP

We now validate and test the above metrics using a point cloud dataset. First, we describe the dataset and how we evaluate the performance of our similarity metrics (Section V-A and V-B, respectively). Then, we run an ablation study to evaluate for each similarity metrics the best performing set of regulators.

TABLE II  
SIMILARITY METRICS: DEFINITIONS, INCLUDED DISTANCE FEATURES AND MEASUREMENTS, REGULATOR AND THRESHOLD VALUES.

Symbol	Definition	Distance Feature and Metric	Regulator values	$G_{th}$
$w_1$	$k_{\alpha}^{(E)}(x^i, x^j)$	$E(x^i, x^j)$	$\alpha = 1$	0.64
$w_2$	$k_{\alpha}^{(L)}(r^i, r^j)$	$L(r^i, r^j)$	$\alpha = 1$	0.80
$w_3$	$k_{\alpha}^{(G)}(p^i, p^j)$	$G(p^i, p^j)$	$\alpha = 1$	0.63
$w_4$	$k_{\alpha}^{(E)}(p^i, p^j)$	$E(p^i, p^j)$	$\alpha = 1$	0.84
$w_5$	$k_{\alpha}^{(E)}(x^i, x^j) \cdot k_{\beta}^{(L)}(r^i, r^j) \cdot k_{\gamma}^{(G)}(p^i, p^j)$	$E(x^i, x^j), L(r^i, r^j), G(p^i, p^j)$	$\alpha = 0.1; \beta = 0.5; \gamma = 1$	0.54
$w_6$	$k_{\alpha}^{(E)}(x^i, x^j) \cdot k_{\beta}^{(L)}(r^i, r^j) \cdot k_{\gamma}^{(E)}(p^i, p^j)$	$E(x^i, x^j), L(r^i, r^j), E(p^i, p^j)$	$\alpha = 0.1; \beta = 0.125; \gamma = 0.2$	0.87
$w_7$	$k_{\alpha}^{(E)}(x^i, x^j) \cdot \beta[\eta(r_i) + \eta(r_j)] \cdot k_{\gamma}^{(G)}(p^i, p^j)$	$E(x^i, x^j), r^i, r^j, G(p^i, p^j)$	$\alpha = 0.25; \beta = 0.5; \gamma = 0.5$	0.60
$w_8$	$k_{\alpha}^{(E)}(x^i, x^j) \cdot \beta[\eta(r_i) + \eta(r_j)] \cdot k_{\gamma}^{(E)}(p^i, p^j)$	$E(x^i, x^j), r^i, r^j, E(p^i, p^j)$	$\alpha = 0.5; \beta = 0.5; \gamma = 0.5$	0.62

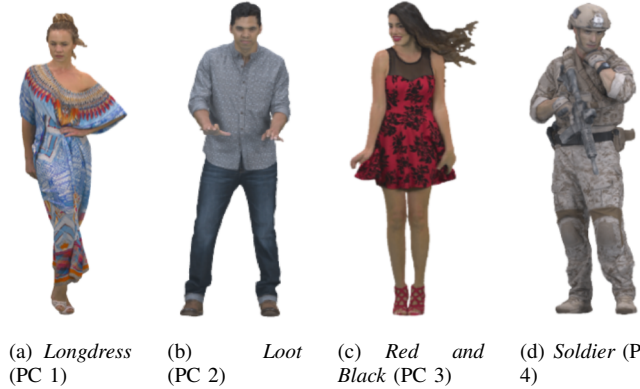


Fig. 3. Human Body Point Clouds [33] content used in the collection of a public available dataset presented in [5].

#### A. Dataset and Methodology

**Dataset.** Existing datasets with user navigation collected while displaying volumetric objects in a 6-DoF environment are still very limited. In the following, we use the open dataset presented in [5]. The dataset is comprised of navigation trajectories of 26 users participating in a visual quality assessment study in VR. For the study, four dynamic point cloud sequences were employed [33], namely *Long dress* (PC1), *Loot* (PC2), *Red and black* (PC3), *Soldier* (PC4) (Fig. 3). Each sequence was distorted at four different bit rate points with two compression algorithms: the anchor used for the MPEG call for proposals, and the upcoming MPEG standard V-PCC. Hidden references were additionally employed in the test, for a total of 36 stimuli. Similarly to what is shown in Fig. 2, a single object of interest was placed in the VR scene, and users were instructed to focus on the volumetric content for the duration of the session and rate its visual quality. Therefore, the navigation data adheres to the assumptions listed in Section III (B).

**Graph Construction.** To implement the graph-based clustering proposed in [20] based on our proposed similarity metrics, we need to construct a binary graph following (2), as described in Section III-C. In short, users with a similarity metric below a threshold value  $G_{th}$  are neighbours in the graph. Hence, the first step is to identify  $G_{th}$ . We empirically evaluate the Receiver Operating Characteristic (ROC) curves per each proposed similarity metric and select the best value. We assess these values based on navigation trajectories collected for the entire dataset above described. As ground-truth for the ROC,

we assumed that two users are attending the same portion of content if their viewports overlap by at least 75% of their total viewed area. The predicted event is instead evaluated using the eight metrics presented in the previous section that approximate the overlap. We selected threshold values to have a probability to correctly classify an event (*i.e.*, True Positive Rate (TPR)) equal to 0.75. In the last column of Table II, we provide the values of  $G_{th}$  corresponding to this TPR for each similarity metric.

#### B. Performance Evaluation Setup

In order to test the validity of our proposed similarity metrics, we consider three performance metrics: averaged *overlap ratio* per cluster, *relevant clustered population*, and *precision*. The first two are more specific to our navigation trajectory in a 6-DoF system, while the latter is a popular index used to evaluate clustering algorithm performance.

**Overlap ratio per cluster:** as defined in Section III-B, the overlap ratio computes the portion in common of displayed content between two users. Therefore, to compare the performance of our detected clusters with the different similarity metrics, we average the overlap ratio among all users who are put in the same group. More formally, given a detected cluster  $C_k$  is defined as follows:

$$O_k = \frac{1}{n_k} \sum_{\substack{i, j \in C_k \\ i \neq j}} O(i, j) \quad (13)$$

where  $i$  and  $j$  are two generic users,  $n_k$  is the cardinality of elements bellowing to clusters  $C_k$ , and  $O(i, j)$  the overlap ratio as defined in Eq.1.

**Relevant clustered population:** the more users are clustered together with a high viewport overlap, the more meaningful are our clusters. Therefore, we consider as a relevant clustered population the sum of users that have been put in clusters with at least 2 other elements.

**Precision:** in a classification task, this index evaluates the portion of elements that are classified correctly and has values between 0 and 1 [34]. More formally:

$$P = \frac{TP}{TP + FP} \quad (14)$$

where True Positive (TP) (False Positive (FP)) is the number of viewers classified correctly (incorrectly) together in a cluster.

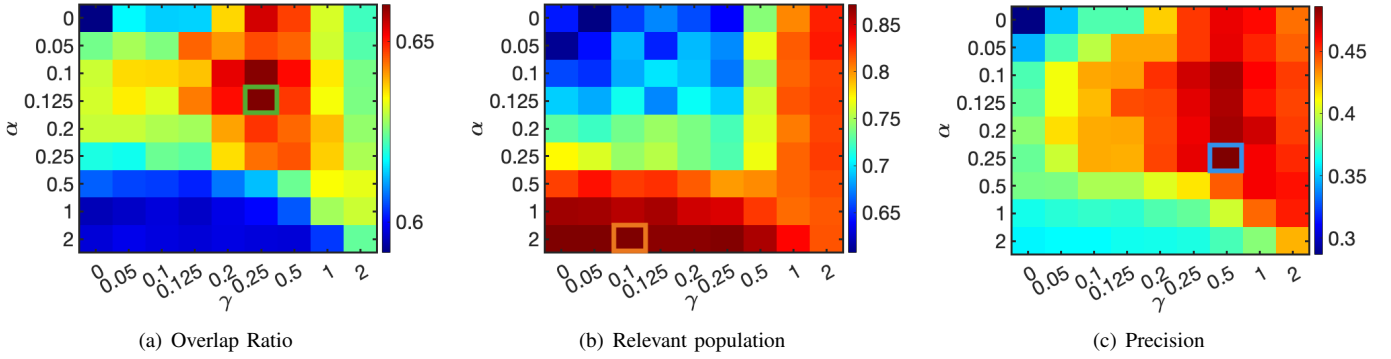


Fig. 4. Example of parameter selection for  $w_7$  with  $\beta = 0.5$ . Values **set 1** selected based on max overlap, **set 2** max clustered users, **set 3** based on precision.

TABLE III  
PARAMETER SELECTIONS AND THEIR PERFORMANCE FOR MULTI-FEATURE METRICS ( $w_5 - w_8$ ).

		$w_5$	$w_6$	$w_7$	$w_8$
<b>set 1</b>	$[\alpha, \beta, \gamma]$	[0.12, 0.125, 0.125]	[0.12, 1, 0.25]	[0.125, 0.5, 0.25]	[0.25, 0.5, 0.2]
	Overlap Ratio	0.63	0.64	0.66	<b>0.69</b>
	Relevant Population	0.82	0.78	0.69	0.62
<b>set 2</b>	$[\alpha, \beta, \gamma]$	[1, 0.05, 0.05]	[0.5, 0.05, 0.05]	[2, 0.5, 0.1]	[2, 0.5, 0.05]
	Overlap Ratio	0.58	0.59	0.60	0.63
	Relevant Population	<b>0.91</b>	0.89	0.87	0.84
<b>set 3</b>	$[\alpha, \beta, \gamma]$	[0.1, 0.5, 1]	[0.1, 0.125, 0.2]	[0.25, 0.5, 0.5]	[0.5, 0.5, 0.5]
	Overlap Ratio	0.63	0.63	0.65	0.66
	Relevant Population	0.83	0.80	0.77	0.74
	Precision	0.45	0.44	<b>0.49</b>	0.48

In our case, two users are identified positively if they are in the same cluster and their viewport overlap is actually over the desired threshold.

### C. Ablation Study

We finally present an ablation study to tune the best set of regulator parameters that maximise the performance of each similarity metric. Equipped with the threshold values per each similarity metrics given in Table II, we run a frame-based clustering to select the best set or sub-set of regulators  $\alpha$ ,  $\beta$  and  $\sigma$ . We test their performance in the following range of values  $[0, 0.05, 0.1, 0.125, 0.2, 0.25, 0.5, 1, 2]$ , based on navigation trajectories collected in the dataset above described; we used the performance metrics described in the previous section such as overlap ratio, precision and relevant population. In detail, we average the final performance of clusters obtained by all similarity metrics over time and across content.

#### Single-feature metrics

For single-feature metrics ( $w_1 - w_4$ ), we notice a very small variance in terms of performance per each similarity metric. Therefore, we decided to select  $\alpha = 1$  for this set of metrics.

#### Multi-feature metrics

More challenging is instead the selection parameters for multi-feature metrics ( $w_5 - w_8$ ). Each similarity metric depends on three parameters:  $\alpha$ ,  $\beta$  and  $\gamma$ . To overcome this, we first select three sets of parameters taking into account only navigation trajectories for reference content: one group of parameters (**set 1**) based on the maximum overlap ratio, the second (**set 2**) depending on the relevant clustered population and the last group (**set 3**) as the one reaching the highest precision. As an

example, we report in Fig. 4 the selection of these three sets of parameters for the similarity metric  $w_7$ . Then, we test these values on all the available trajectories included in the analysed dataset to finally select the best set of parameters. Table III provides all the performance of the multi-feature similarity metrics obtained by the three selected sets of parameters. Since there is no particular configuration that outperforms in terms of overlap ratio, relevant population and precision, we decided to select all regulators selected in **set 3**. This configuration indeed ensures a good balance of overlap ratio and relevant population for all the similarity metrics and ensure the highest value of precision. In Table II, we provide the resulting regulator values used in the following analysis.

## VI. ANALYSIS AND DISCUSSION

Equipped with the similarity metrics, the corresponding values of regulator parameters and threshold  $G_{th}$  reported in Table II, we now conduct our validation study. In detail, we focus on analysing navigation trajectories experienced with non-distorted content.

### A. Frame-Based Analysis

As first step, we implement a frame-based analysis (i.e., frame-based clustering) to visually verify the performance of the detected clusters in the different settings of similarities. Fig. 5 shows the clusters detected using the ground-truth metric  $O$  to construct the graph (Fig. 5 (a)) with the ones given based on each proposed similarity metric (Fig. 5 (b-i)), for frame 50 of sequence PC1. In particular, each user is

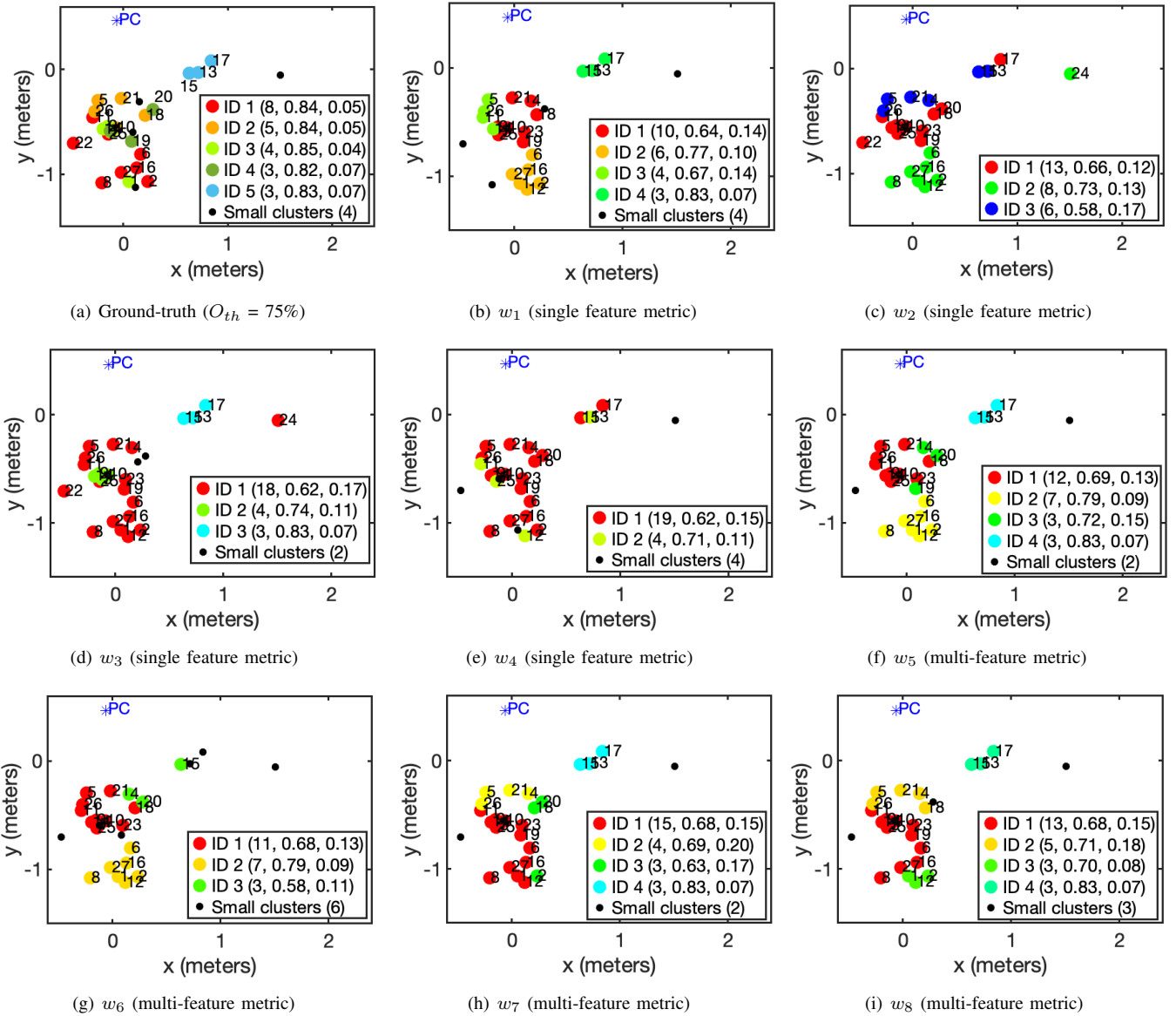


Fig. 5. Cluster results in frame 50 of sequence PC1 (*Longdress*). Each dot represents a user on the virtual floor while the blue star stands for the volumetric content. In the legend, per each cluster with more than 2 users are reported on brackets the following values: the number of users included in the same cluster, averaged pairwise viewport overlap and corresponding variance within the cluster.

represented by a point on the VR floor which is coloured based on the assigned ID cluster, whereas the volumetric content is symbolised by a blue star. For each relevant cluster (*i.e.*, cluster with more than 2 users), we provide in the legend the following results: number of users inside the cluster, the average and variance of the overlap ratio among all users within the cluster. Finally, we represent the remaining users which are in either single or couple-cluster as black points; the total number of these users is also provided in the legend as “Small clusters (total number of non-relevant clusters)”. We can notice that single feature metrics, Fig. 5 (b-e), have the tendency to create very populated clusters but with a low overlap ratio. For instance,  $w_3$  and  $w_4$  generate a main big cluster with 18 and 19 users, respectively, while the corresponding overlap ratio drops drastically to 0.62. The only exception is given by  $w_1$ , which generates a variable set of clusters with consistent values of overlap ratio, over 0.64. Let us now consider as an

example the users 13, 15 and 17, which in the ground-truth case (Fig. 5 (a)) form their own cluster (*i.e.*, ID 5) with a high overlap ratio (0.83), and user 24, who is quite isolated from other users and belongs to a single cluster. We can notice that  $w_2$  and  $w_4$  fail in detecting the group of users 13, 15 and 17 as similar, dividing them instead in different clusters. On the other hand,  $w_3$  detects this similarity but puts user 24 in a relevant cluster (ID 1). From these observations, we can notice that the projection of the viewport centre on the volumetric content, which forms the basis of  $w_3$  and  $w_4$ , is not sufficient to correctly identify similar users. Analogously, considering only the difference in terms of the relative distance between the user and volumetric content, as done in  $w_2$ , does not allow to detect similarity among users. Thus, the most promising metric in this group seems to be  $w_1$ , which is based on the user position on the virtual floor.

The last group of Fig. 5 (f-i) shows clusters based on multi-

TABLE IV  
RESULTS IN TERMS OF AVERAGED AND STANDARD DEVIATION PER EACH PERFORMANCE METRIC ACROSS THE ENTIRE DATASET.

Metrics		$w_1$	$w_2$	$w_3$	$w_4$	$w_5$	$w_6$	$w_7$	$w_8$
PC1	Overlap Ratio	0.68 $\pm$ 0.05	0.65 $\pm$ 0.04	0.66 $\pm$ 0.04	0.68 $\pm$ 0.07	0.70 $\pm$ 0.05	0.71 $\pm$ 0.05	0.70 $\pm$ 0.05	<b>0.72 <math>\pm</math> 0.06</b>
	Relevant Population	0.85 $\pm$ 0.04	<b>0.94 <math>\pm</math> 0.03</b>	0.92 $\pm$ 0.05	0.84 $\pm$ 0.08	0.83 $\pm$ 0.06	0.83 $\pm$ 0.07	0.83 $\pm$ 0.06	0.83 $\pm$ 0.07
	Precision	0.44 $\pm$ 0.06	0.35 $\pm$ 0.05	0.39 $\pm$ 0.07	0.30 $\pm$ 0.06	0.47 $\pm$ 0.07	<b>0.49 <math>\pm</math> 0.08</b>	0.46 $\pm$ 0.07	0.44 $\pm$ 0.10
PC2	Overlap Ratio	0.57 $\pm$ 0.08	0.53 $\pm$ 0.09	0.54 $\pm$ 0.12	0.54 $\pm$ 0.11	0.59 $\pm$ 0.08	0.58 $\pm$ 0.08	0.59 $\pm$ 0.12	<b>0.60 <math>\pm</math> 0.10</b>
	Relevant Population	0.80 $\pm$ 0.07	<b>0.92 <math>\pm</math> 0.06</b>	0.83 $\pm$ 0.07	0.89 $\pm$ 0.06	0.80 $\pm$ 0.10	0.81 $\pm$ 0.07	0.72 $\pm$ 0.08	0.73 $\pm$ 0.06
	Precision	0.45 $\pm$ 0.06	0.28 $\pm$ 0.08	0.31 $\pm$ 0.08	0.27 $\pm$ 0.08	0.47 $\pm$ 0.09	0.42 $\pm$ 0.08	<b>0.54 <math>\pm</math> 0.08</b>	<b>0.54 <math>\pm</math> 0.12</b>
PC3	Overlap Ratio	0.65 $\pm$ 0.06	0.60 $\pm$ 0.07	0.64 $\pm$ 0.05	0.68 $\pm$ 0.06	0.65 $\pm$ 0.06	0.65 $\pm$ 0.06	0.68 $\pm$ 0.05	<b>0.69 <math>\pm</math> 0.05</b>
	Relevant Population	0.82 $\pm$ 0.07	<b>0.93 <math>\pm</math> 0.05</b>	0.88 $\pm$ 0.06	0.82 $\pm$ 0.08	0.84 $\pm$ 0.06	0.81 $\pm$ 0.07	0.72 $\pm$ 0.07	0.70 $\pm$ 0.07
	Precision	0.48 $\pm$ 0.11	0.36 $\pm$ 0.08	0.39 $\pm$ 0.07	0.39 $\pm$ 0.06	0.49 $\pm$ 0.11	0.49 $\pm$ 0.10	0.52 $\pm$ 0.08	<b>0.55 <math>\pm</math> 0.08</b>
PC4	Overlap Ratio	0.60 $\pm$ 0.04	0.52 $\pm$ 0.06	0.55 $\pm$ 0.03	0.59 $\pm$ 0.06	0.59 $\pm$ 0.04	0.58 $\pm$ 0.05	0.61 $\pm$ 0.04	<b>0.66 <math>\pm</math> 0.05</b>
	Relevant Population	0.82 $\pm$ 0.07	<b>0.92 <math>\pm</math> 0.05</b>	0.90 $\pm$ 0.08	0.86 $\pm$ 0.08	0.83 $\pm$ 0.08	0.77 $\pm$ 0.07	0.80 $\pm$ 0.07	0.71 $\pm$ 0.08
	Precision	0.35 $\pm$ 0.06	0.22 $\pm$ 0.04	0.31 $\pm$ 0.06	0.25 $\pm$ 0.07	0.38 $\pm$ 0.07	0.38 $\pm$ 0.09	<b>0.42 <math>\pm</math> 0.06</b>	<b>0.42 <math>\pm</math> 0.07</b>
All PCs	Overlap Ratio	0.62 $\pm$ 0.06	0.57 $\pm$ 0.06	0.60 $\pm$ 0.06	0.62 $\pm$ 0.07	0.63 $\pm$ 0.06	0.63 $\pm$ 0.06	0.65 $\pm$ 0.06	<b>0.66 <math>\pm</math> 0.06</b>
	Relevant Population	0.82 $\pm$ 0.06	<b>0.93 <math>\pm</math> 0.05</b>	0.88 $\pm$ 0.07	0.85 $\pm$ 0.08	0.83 $\pm$ 0.07	0.80 $\pm$ 0.07	0.77 $\pm$ 0.07	0.74 $\pm$ 0.07
	Precision	0.43 $\pm$ 0.07	0.30 $\pm$ 0.06	0.35 $\pm$ 0.07	0.30 $\pm$ 0.07	0.45 $\pm$ 0.09	0.45 $\pm$ 0.09	<b>0.49 <math>\pm</math> 0.07</b>	0.48 $\pm$ 0.09

feature similarity metrics. In all these settings, a total of four main clusters are detected, except for  $w_6$  that leads to three clusters, as shown in Fig. 5 (g). The latter detects the highest number of small clusters (6) while being the only one that does not identify users 13, 15 and 17 as belonging to the same cluster. On the contrary, the other three metrics  $w_5$ ,  $w_7$  and  $w_8$  detect a main cluster and three smaller clusters with a consistent overlap ratio. For instance, the resulting clusters based on  $w_5$  have an overlap ratio always bigger than 0.69 and only two users fall in small clusters. Overall, multi-functional metrics appear to be better suited to detect similar users than previous ones, with the exception of  $w_6$ . This is expected as higher degrees of freedom are given to users, the more challenging is the system, and thus users similarity to detect.

Instead of looking at one frame only, we now analyse the per-frame clustering technique providing in Table IV the performance averaged over time and corresponding standard deviation. In detail, we show the average and standard deviation of performance metrics described in Section V-B across the entire analysed dataset. To be noted that clusters based on  $w_2$  are able to group in the relevant clusters the majority of the population in all the analysed PCs (reaching the maximum value of 0.94 in PC1) to the detriment of precision, which falls to values between 0.22 and 0.35. As already shown in the previous investigation, the most promising similarity metrics in terms of precision and overlap ratio are both  $w_7$  and  $w_8$  followed by  $w_5$ . These outperform the other weights in all PCs, ensuring an overlap ratio within the same cluster with values in the range of 0.59 and 0.70 for  $w_7$ , 0.60 and 0.72 for  $w_8$ . Similarly, the values of precision are always over 0.42 for both  $w_7$  and  $w_8$ . The only exception is in PC1, where the best performing metric in terms of precision is  $w_6$ , which for the other contents cases is always the worst performing among multi-functional metrics.

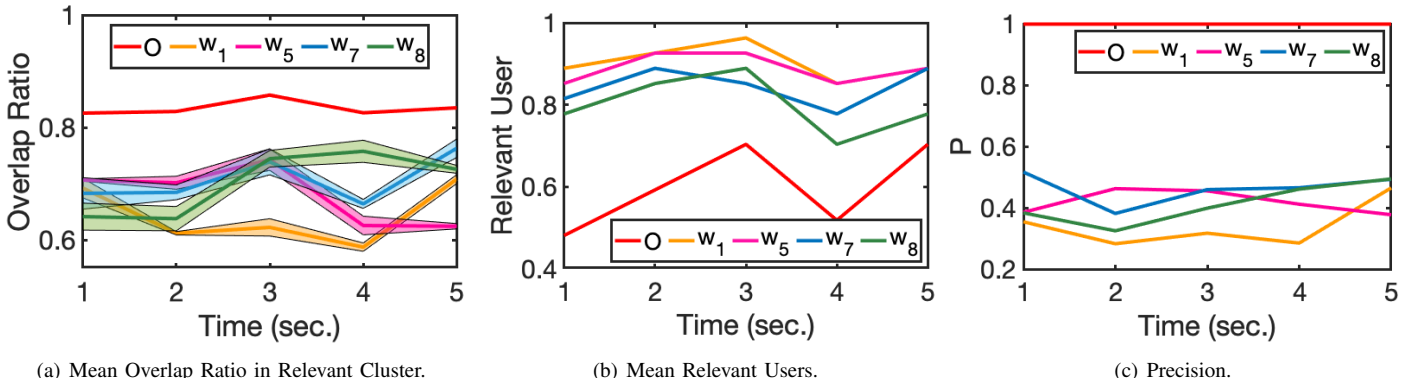
### B. Trajectory-Based analysis

Given the above remarks, we now analyse the performance metrics over time, taking into account only  $w_1$ ,  $w_5$ ,  $w_7$ , and  $w_8$ . Indeed, we decide to select the best performing similarity metrics in the previous investigation ( $w_5$ ,  $w_7$  and  $w_8$ ). To have a fair comparison, we also keep the most promising among the single-feature metrics,  $w_1$ . We compute clique-based clusters

over a time window of 1s (*i.e.*, chunk) and a time similarity threshold of 0.8s. At each chunk, we evaluate the average overlap ratio per relevant cluster (*i.e.*, cluster with at least two elements), the average of the relevant population and the precision of detected clusters. As an example, we show these results per sequence PC1 (*Longdress*) as functions of time for each similarity metric under consideration in each subplot of Fig. 6. In the figures, we also add the performance of clusters detected by the ground-truth metric  $O$  (*i.e.*, red line). We observe that all similarity metrics reach an average overlap ratio within clusters between 0.6 and 0.75 (Fig. 6 (a)). However, clusters based on  $w_1$  appear to have lower performance than other metrics which are quite similar, although with a slight predominance of  $w_7$ . In terms of relevant users (Fig. 6 (b)), it is worth noting that all the proposed similarity metrics generate bigger clusters than the ground-truth metric, which considers only half of the population as relevant. In more detail, the clusters resulting from  $w_1$ ,  $w_5$  and  $w_8$  put in relevant clusters 0.8 of the entire population for all the sequence time. Finally, in terms of precision as highlighted in Fig. 6 (c) the only similarity metric that generated clusters with P over to 0.4 in the entire sequence is  $w_7$ . These investigations show that similarity metrics based on multi-feature, such as  $w_7$  and  $w_8$ , are more promising for detecting users with a similar behaviour while experiencing volumetric content. In summary, from this validation analysis, we can conclude the following:

- Overall, *multi-feature metrics* are more precise in detecting users with similar behaviour (in terms of displayed content) both in a frame- and chunk-based analysis;
- In particular, in spite of the slightly more complex formulation,  $w_7$  and  $w_8$  are robust and easy-to-use metrics that ensure a robust and reliable behavioural analysis via clustering tools;
- On the contrary, metrics based only on a single feature (*i.e.*, *single-feature metrics*) are not sufficient to correctly identify similar users;
- The only exception among single-feature metrics is  $w_1$  which is based only on the position of the user on the floor. Despite its simplicity, this metric is comparable with multi-feature metrics. Hence, it can be used for an easy-to-implement preliminary behavioural analysis.

These considerations have been built on point clouds with



(a) Mean Overlap Ratio in Relevant Cluster.

(b) Mean Relevant Users.

(c) Precision.

Fig. 6. Spherical clustering over time (chunk = 1 sec.) results per sequence PC1 (*Longdress*): comparison between Ground-truth, and a subset of proposed metrics ( $w_1$ ,  $w_5$ ,  $w_7$  and  $w_8$ ).

human body. We leave further investigations across multiple types of content for future works.

## VII. CASE STUDY

The above study has been carried out with a dataset only and we are therefore interested in understanding if insights from the above study could be applied to other human-like datasets. To show that our study generalises to datasets, we now investigate the proposed metrics on the dataset presented in [18]. Authors have collected navigation trajectories of 20 users while displaying volumetric content in an Augmented Reality (AR) scenario. Similarly to the previously analysed dataset presented in Section V-A, a single object of interest was placed in the scene. Specifically, two dynamic volumetric human body sequences represented as 3D meshes with texture information were used: *Nico* (VV1) and *Sir Frederic* (VV2) in Figure 7, respectively. In order to conduct our study, both the sequences were kindly made available by Volograms upon request [35], [36]. The navigation data have been collected in a remote scenario through an Android AR application, which allowed users to display the volumetric content from any desired location and portable device (e.g., smartphone). Participants were also free to display the volumetric content how they most preferred. Thus, the main differences with the previously analysed dataset are the following: the different format of volumetric content (3D mesh instead of point cloud), different immersive scenario (AR instead of VR application) and the heterogeneity of viewing devices (any smartphone device instead of a specific HMD). In particular, the 3D mesh content does not allow for a simple formulation of the overlap ratio as we have described it in Section III-B. For consistency, we convert the sequences from 3D meshes to point clouds by discarding edge information and only keeping vertices as points; we discuss the inherent challenges to define our ground-truth metric in Section VIII.

Similarly to our previous investigations, we now apply to this new scenario the spherical clustering based on the subset of best-performing feature metrics, such as  $w_1$ ,  $w_5$ ,  $w_7$  and  $w_8$ . We evaluate clusters in chunks of length 1s with a time similarity threshold of 0.8s and the threshold values  $G_{th}$  reported in Table II. At each chunk, we compute the average overlap ratio per relevant cluster (*i.e.*, cluster with at least

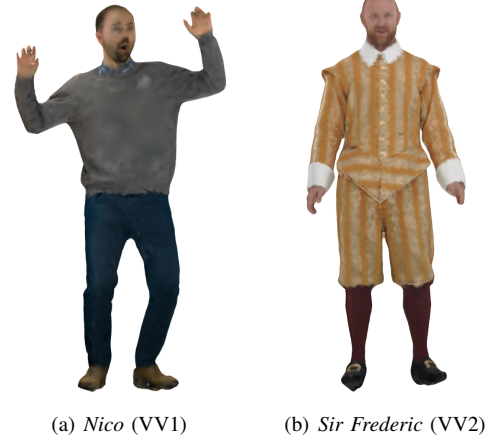


Fig. 7. Volumetric Human Body sequences [35] used in the AR experiment presented in [18]

two elements), the average of the relevant population and the precision of the detected clusters. Fig. 8 shows these results as a function of time per each selected similarity metric, in particular, the first row refers to *Nico* (VV1) while the second one to *Sir Frederic* (VV2). Since viewers were allowed to drop the AR experience at any desired time, in the following we consider only the time window in which 75% of the user population (15 out of 20 viewers) are still in the experiment: 63 and 83 seconds, respectively for VV1 and VV2. We observe that both the sequences have an initial moment of adjustment where viewers are displaying different portions of the content. This is detected by clusters based on the overlap ratio (*i.e.*, red line) which do not have a consistent pairwise overlap. For instance, Fig. 8 (a) shows in the first 40s of the immersive experience for VV1 the average of overlap ratio within the main detected clusters has up and down for all the metrics, included the ground-truth. However, this behaviour stabilises around 40s when the overlap ratio for the ground-truth metric converge to 1. Similarly, the performance metric detected by  $w_1$  and  $w_8$  reaches values above 0.6 with a very low variance for both the metrics. On the contrary, the overlap ratio of cluster detected by  $w_5$  and  $w_7$  has values below 0.5 and a more consistent variance over time. Indeed, these metrics in terms of relevant users (Fig. 8 (b)) generate bigger clusters compared to the ground-truth metric. In particular,

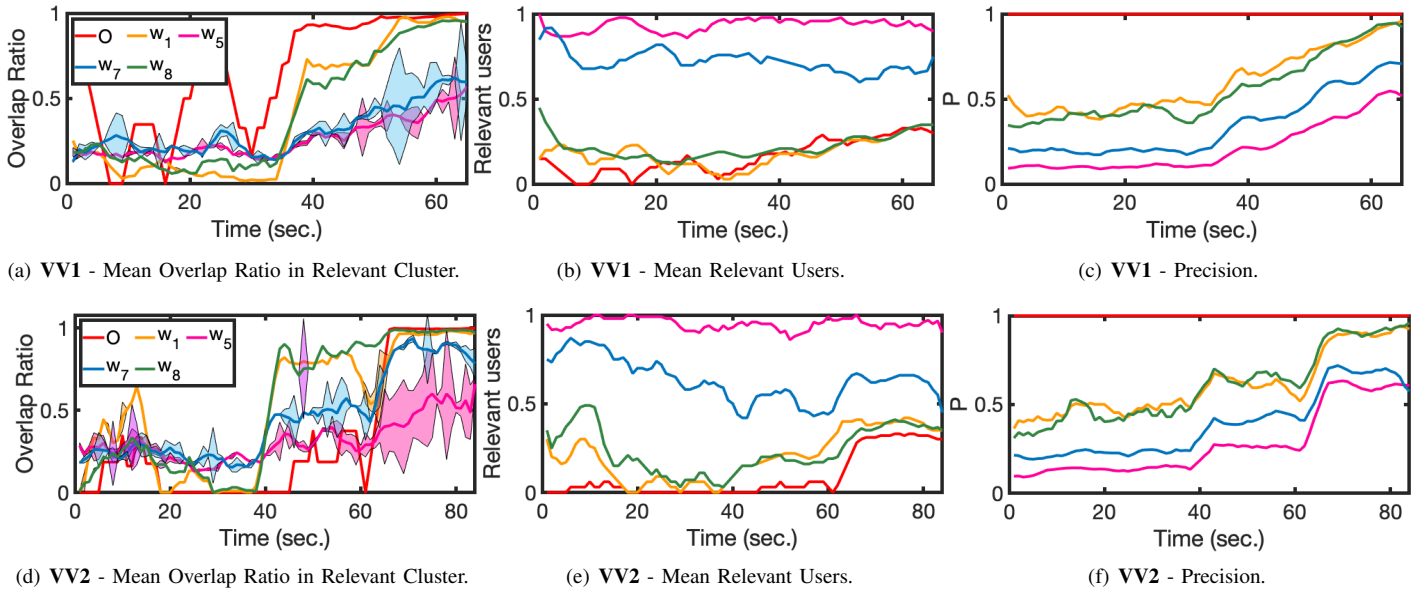


Fig. 8. Spherical clustering over time (chunk = 1 sec.) results per sequence VV1 (*Nico*) and VV2 (*Sir Fredrick*): performance comparison between ground-truth, and a subset of proposed metrics ( $w_1, w_5, w_7$  and  $w_8$ ).

$w_5$  considers almost the entire population at any given time in a big cluster, which is quite the opposite behaviour to the ground-truth metric. This metric indeed generates small relevant clusters most of the time; clusters based on  $w_1$  and  $w_8$  follow a very similar trend. These two metrics are also the best performing in terms of precision, as shown in Fig. 8 (c) with values always above 0.4. A similar general behaviour is also observable for VV2 in the second line of Fig. 8. In this volumetric content, users explore more randomly during the first minute of the experience to end up having similar behaviour, in fact, clusters have a consistent overlap ratio (Fig. 8 (d)). As in the previous example, similarity metrics  $w_1$  and  $w_8$  are more precise in reflecting the ground-truth behaviour and thus, detecting viewers with similar behaviour and putting them within the same clusters. Finally, it is worth noticing that between 40 and 60 seconds, all the similarity metrics reach a higher overlap ratio compared to the ground-truth performance, in particular, metrics  $w_1$  and  $w_8$ . This opens new questions to be further investigated as discussed in the following section.

### VIII. DISCUSSION AND FUTURE WORK

We presented the main challenges of user behavioural analysis in a 6-DoF system due to the new settings and the added locomotion functionalities. However, behavioural analysis of 6-DoF users is not considered in the literature yet; as such, there is no reference metric available to detect viewers who are displaying the same portion of the content. Thus, we had to define a general ground-truth user similarity metric, such as *overlap ratio*. To be as general as possible, we established the overlap as the percent of points displayed in common by two users. This is fairly straightforward, albeit time-consuming, to compute for point cloud contents, in which each point is rendered separately. For other types of volumetric contents, determining the overlap ratio is not as simple. Considering

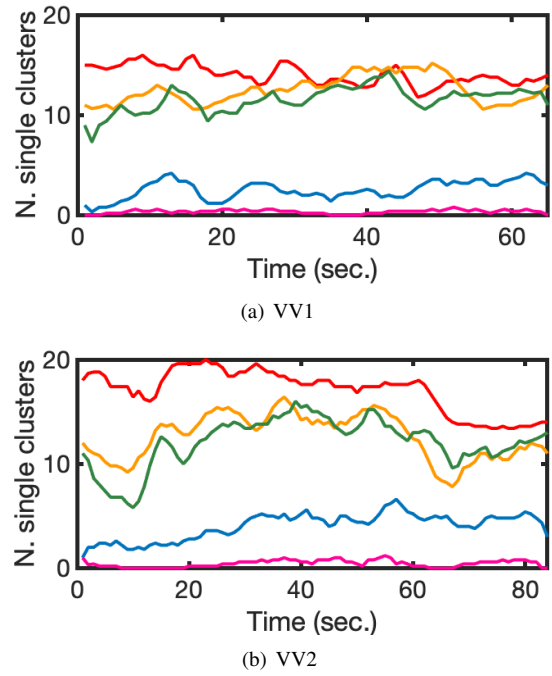


Fig. 9. Single-user cluster per sequence VV1 (*Nico*) and VV2 (*Sir Fredrick*) obtained via spherical clustering based on overlap ratio, and a subset of proposed similarity metrics ( $w_1, w_5, w_7$  and  $w_8$ ).

the number of vertexes that fall into a given frustum could lead to misleading results when large faces between sparsely distributed vertexes are present. Moreover, the metric requires to render each volumetric video at any given time and for each viewer, making its computation not trivial and intensely time-consuming. To overcome this issue and to assess users similarity in a simple and objective way, we investigate several similarity metrics considering different distance features and measurements. In detail, we investigate different features or combinations of them which consider users location in the

virtual space and their viewing direction. First, we validate and test our similarity metrics via a clique-based clustering tool proposed for 3-DoF scenario on real navigation trajectory collected in a 6-DoF VR environment. Our extensive analysis shows that metrics based on multi-features better model and thus, detect similarity among users, reaching encouraging values of both overlap ratio and precision. Therefore, we tested their performance on a different kind of 6-DoF navigation trajectories. In this second dataset, viewers displayed volumetric content in an AR scenario through smartphones. Therefore, even if users were enabled with the same 6-DoF locomotion settings, the viewing device and the FoV were different. Despite these differences, our proposed similarity metrics are still good at identifying viewers who are displaying similar content. In this context not only a multi-feature metric is outperforming the others, but also the simplest one which is based only on the users location in the virtual space. This opens the gate to further investigations aimed at detecting user behavioural differences in a 6-DoF experience done in VR and AR settings. These are indeed essential to be exploited in efficient user-centric solutions for both immersive systems. Finally, it is worth mentioning that our ground-truth metric of similarity is very tight in detecting similar users, especially in an AR scenario. As an example, Fig. 9 shows the number of single clusters detected over time by the overlap ratio (*i.e.*, red line) and the sub-set of most performing similarity metrics for both the volumetric sequences of the second analysed dataset. In particular, in VV2 (Fig. 9 (b)), the clique-based clustering based on the overlap ratio does not detect similar users such that the majority of the population are put in a single cluster. Therefore, further analysis is needed to test if in this scenario a different overlap threshold better model similarity among users.

## IX. CONCLUSION

In this paper, we have presented similarity metrics to enable behavioural analysis of users while exploring a 6-DoF immersive content. We were interested in modelling similarities among users *observing the same volumetric content*. In our previous work [19], we have shown that the way in which users interact within a 3- and 6-DoF scenario is fundamentally different preventing a straightforward extension of current 3-DoF algorithms to 6-DoF. Therefore, in this article we advanced the state-of-the-art, proposing novel similarity metrics taking into account the new physical settings and locomotion functionalities given to users. Our results showed that solutions that consider both user position and viewing direction are promising to correctly detect users with a similar behaviour while experiencing volumetric content. We have also demonstrated the robustness and versatility of these metrics, which preserve good performance on navigation trajectories collected in a 6-DoF AR scenario.

## REFERENCES

- [1] P. Cipresso, I. A. C. Giglioli, M. A. Raya, and G. Riva, “The past, present, and future of virtual and augmented reality research: a network and cluster analysis of the literature,” *Frontiers in psychology*, vol. 9, p. 2086, 2018.
- [2] M. Xu, C. Li, S. Zhang, and P. Le Callet, “State-of-the-art in 360 video/image processing: Perception, assessment and compression,” *IEEE Journal of Selected Topics in Signal Processing*, vol. 14, no. 1, pp. 5–26, 2020.
- [3] S. Schwarz, M. Preda, V. Baroncini, M. Budagavi, P. Cesar, P. A. Chou, R. A. Cohen, M. Krivokuća, S. Lasserre, Z. Li *et al.*, “Emerging MPEG standards for point cloud compression,” *IEEE Journal on Emerging and Selected Topics in Circuits and Systems*, vol. 9, no. 1, pp. 133–148, 2018.
- [4] J. Harth, A. Hofmann, M. Karst, D. Kempf, A. Ostertag, I. Przemus, and B. Schaefermeyer, “Different types of users, different types of immersion: A user study of interaction design and immersion in consumer virtual reality,” *IEEE Consumer Electronics Magazine*, vol. 7, no. 4, pp. 36–43, 2018.
- [5] S. Subramanyam, I. Viola, A. Hanjalic, and P. Cesar, “User Centered Adaptive Streaming of Dynamic Point Clouds with Low Complexity Tiling,” in *Proceedings of the 28th ACM International Conference on Multimedia*, 2020, pp. 3669–3677.
- [6] J. Park, P. A. Chou, and J.-N. Hwang, “Rate-utility optimized streaming of volumetric media for augmented reality,” *IEEE Journal on Emerging and Selected Topics in Circuits and Systems*, vol. 9, no. 1, pp. 149–162, 2019.
- [7] S. Rossi, C. Ozcinar, A. Smolic, and L. Toni, “Do Users Behave Similarly in VR? Investigation of the User Influence on the System Design,” *ACM Transactions on Multimedia Computing, Communications, and Applications*, 2020.
- [8] J. Van der Hooft, T. Wauters, F. De Turck, C. Timmerer, and H. Hellwagner, “Towards 6-DoF HTTP adaptive streaming through point cloud compression,” in *Proceedings of the 27th ACM International Conference on Multimedia*, 2019.
- [9] B. Han, Y. Liu, and F. Qian, “Vivo: Visibility-aware mobile volumetric video streaming,” in *Proceedings of the 26th Annual International Conference on Mobile Computing and Networking*, 2020, pp. 1–13.
- [10] X. Corbillon, F. De Simone, and G. Simon, “360-degree video head movement dataset,” in *Proceedings of the 8th ACM on Multimedia Systems Conference*, 2017.
- [11] E. J. David, J. Gutiérrez, A. Coutrot, M. P. Da Silva, and P. L. Callet, “A dataset of head and eye movements for 360 videos,” in *Proceedings of the 9th ACM Multimedia Systems Conference*, 2018, pp. 432–437.
- [12] S. Fremerey, A. Singla, K. Meseberg, and A. Raake, “AVtrack360: An open dataset and software recording people’s head rotations watching 360° videos on an HMD,” in *Proceedings of the 9th ACM Multimedia Systems Conference*, 2018, pp. 403–408.
- [13] A. T. Nasrabadi, A. Samiee, A. Mahzari, R. P. McMahan, R. Prakash, M. C. Farias, and M. M. Carvalho, “A taxonomy and dataset for 360° videos,” in *Proceedings of the 10th ACM Multimedia Systems Conference*, 2019, pp. 273–278.
- [14] V. Sitzmann, A. Serrano, A. Pavel, M. Agrawala, D. Gutierrez, B. Masia, and G. Wetzstein, “Saliency in VR: How do people explore virtual environments?” in *IEEE Transactions on Visualization and Computer Graphics*, 2018.
- [15] S. Rossi and L. Toni, “Understanding user navigation in immersive experience: an information-theoretic analysis,” in *Proceedings of the 12th ACM International Workshop on Immersive Mixed and Virtual Environment Systems*, 2020.
- [16] E. Alexiou, N. Yang, and T. Ebrahimi, “PointXR: A toolbox for visualization and subjective evaluation of point clouds in virtual reality,” in *2020 Twelfth International Conference on Quality of Multimedia Experience*. IEEE, 2020, pp. 1–6.
- [17] S. Subramanyam, J. Li, I. Viola, and P. Cesar, “Comparing the Quality of Highly Realistic Digital Humans in 3DoF and 6DoF: A Volumetric Video Case Study,” in *IEEE Conference on Virtual Reality and 3D User Interfaces*, 2020.
- [18] E. Zerman, R. Kulkarni, and A. Smolic, “User behaviour analysis of volumetric video in augmented reality,” in *13th International Conference on Quality of Multimedia Experience*. IEEE, 2021, pp. 129–132.
- [19] S. Rossi, I. Viola, L. Toni, and P. Cesar, “A New Challenge: Behavioural Analysis Of 6-DOF User When Consuming Immersive Media,” in *2021 IEEE International Conference on Image Processing*. IEEE, 2021, pp. 3423–3427.
- [20] S. Rossi, F. De Simone, P. Frossard, and L. Toni, “Spherical clustering of users navigating 360 content,” in *IEEE International Conference on Acoustics, Speech and Signal Processing*, 2019.
- [21] H. Jun, M. R. Miller, F. Herrera, B. Reeves, and J. N. Bailenson, “Stimulus sampling with 360-videos: Examining head movements, arousal, presence, simulator sickness, and preference on a large sample of

- participants and videos,” *IEEE Transactions on Affective Computing*, pp. 1–1, 2020.
- [22] J. Bermejo-Berros and M. A. G. Martínez, “The relationships between the exploration of virtual space, its presence and entertainment in virtual reality, 360° and 2d,” *Virtual Reality*, pp. 1–17, 2021.
- [23] A. T. Nasrabadi, A. Samiei, and R. Prakash, “Viewport prediction for 360 videos: a clustering approach,” in *Proceedings of the 30th ACM Workshop on Network and Operating Systems Support for Digital Audio and Video*, 2020, pp. 34–39.
- [24] D. D. R. Moraes, L. S. Althoff, R. Prakash, M. M. Carvalho, and M. C. Farias, “A content-based viewport prediction model,” in *Electronic Imaging*, vol. 2021, no. 9, 2021.
- [25] D. Freeman, S. Reeve, A. Robinson, A. Ehlers, D. Clark, B. Spanlang, and M. Slater, “Virtual reality in the assessment, understanding, and treatment of mental health disorders,” *Psychological medicine*, vol. 47, no. 14, pp. 2393–2400, 2017.
- [26] C. N. Geraets, E. C. van der Stouwe, R. Pot-Kolder, and W. Veling, “Advances in immersive virtual reality interventions for mental disorders—a new reality?” *Current opinion in psychology*, 2021.
- [27] C. Swindells, B. A. Po, I. Hajshirmohammadi, B. Corrie, J. Dill, B. Fisher, and K. Booth, “Comparing CAVE, wall, and desktop displays for navigation and wayfinding in complex 3D models,” in *IEEE Proceedings Computer Graphics International*, 2004.
- [28] E. D. Ragan, S. Scerbo, F. Bacim, and D. A. Bowman, “Amplified head rotation in virtual reality and the effects on 3d search, training transfer, and spatial orientation,” *IEEE transactions on visualization and computer graphics*, vol. 23, no. 8, pp. 1880–1895, 2016.
- [29] H. Creagh, “Cave automatic virtual environment,” in *Proceedings: Electrical Insulation and Electrical Manufacturing and Coil Winding Technology Conference*, 2003, pp. 499–504.
- [30] W. Chen, A. Plancoulaine, N. Férey, D. Touraine, J. Nelson, and P. Bourdot, “6DoF navigation in virtual worlds: comparison of joystick-based and head-controlled paradigms,” in *Proceedings of the 19th ACM Symposium on Virtual Reality Software and Technology*, 2013.
- [31] S. Rossi, I. Viola, J. Jansen, S. Subramanyam, L. Toni, and P. Cesar, “Influence of Narrative Elements on User Behaviour in Photorealistic Social VR,” in *Proceedings of the International Workshop on Immersive Mixed and Virtual Environment Systems*. ACM, 2021, p. 1–7.
- [32] L. Stankovic, D. P. Mandic, M. Dakovic, I. Kisil, E. Sejdic, and A. G. Constantinides, “Understanding the basis of graph signal processing via an intuitive example-driven approach [lecture notes],” *IEEE Signal Processing Magazine*, vol. 36, no. 6, pp. 133–145, 2019.
- [33] M. Krivokuća, P. Chou, and P. Savill, “8i voxelized surface light field (8ivslf) dataset,” in *ISO/IEC JTC1/SC29/WG11 MPEG, input document m42914*, 2018.
- [34] T. Fawcett, “An introduction to ROC analysis,” *Pattern recognition letters*, vol. 27, no. 8, pp. 861–874, 2006.
- [35] R. Pagés, E. Zerman, K. Amplianitis, J. Ondřej, and A. Smolic, “Volograms & V-SENSE Volumetric Video Dataset,” *ISO/IEC JTC1/SC29/WG07 MPEG2021/m56767*, 2021.
- [36] Volograms, “Volograms homepage.” [Online]. Available: <https://www.volograms.com/>